CAVITATION EFFECTS ON THE PRESSURE DISTRIBUTION OF A SQUEEZE FILM DAMPER BEARING

Fouad Y. Zeidan and John M. Vance
Department of Mechanical Engineering
Texas A&M University
College Station, Texas 77843, U.S.A.

High speed motion pictures have revealed several operating regimes in a squeeze film damper. Pressure measurements corresponding to these distinct regimes were made to examine their effect on the performance of such dampers. Visual observation also revealed the means by which the pressure in the feed groove showed higher amplitudes than the theory predicts. Comparison between vapor and gaseous cavitation are made based on their characteristic pressure wave, and the effect this has on the total force and its phase.

INTRODUCTION

Squeeze film damper bearings have become an integral part of most modern jet engines. Their performance prediction is an important part of the rotordynamic analysis which requires an accurate representation of the dynamic forces generated within the damper. When operating in a cavitated regime and at high eccentricities, the bearing exhibits a non-linear hardening spring behaviour. Mohan, Rabinwitz, and Hahn [1-3] investigated the effect this nonlinearity has on the synchronous response of rigid and flexible rotors. Nikolajsen and Holmes [4] reported the existence of non-synchronous vibrations which was witnessed on experimental as well as on industrial installations. Since most if not all of squeeze film dampers in actual installations operate in a cavitated mode, and in light of the alarming characteristics described in [1-4], it becomes very important to be capable of properly predicting the type and extent of cavitation. The resulting influence on the radial and tangential forces generated by the squeeze film should also be examined.

The treatment of cavitation in squeeze film damper bearings has for the

Portions of the work reported here were supported by General Electric-Aircraft Engine Business Group; technical monitor, A. F. Storace

most part been an extension of the treatment of cavitation in steadily loaded journal bearings. The experimental work of Cole and Hughes [5] on a bearing subjected to a rotating load, led them to believe that the region of cavitation moved around the bearing and was similar to that in a steadily loaded journal bearing. Thus the boundary conditions often utilized in the analysis of journal bearings were directly applied to dynamic and squeeze film damper bearings. White [6] provided experimental evidence that contradicted the assumption stated above. He reported cavitation bubbles that persisted in the high pressure region when operating at eccentricities larger than 0.3. Hibner and Basnal [7] showed significant deviations in their measurements from predictions of the theory as the cavitation extent in the damper increased. Other investigators [8-10] also experienced significant deviations between theory and measurements. The deviations were attributed to various reasons which ranged from inertial effects that are commonly neglected in the classical lubrication theory, to the presence of turbulence, vorticity, and rotordynamic effects. While it is clear that there is a lack of consensus on the exact source for the deviations, there is a general agreement on the notion that cavitation in squeeze film dampers is far more complex than that in steadily loaded journal bearings. Squeeze film dampers usually have seals to limit side leakage, and in general have different configurations of oil feed such as circumferential grooves or inlet holes. These features make the analysis and specification of the boundary conditions a much more complex problem than that associated with rotating journal bearings.

Partly because of the complexities associated with squeeze film dampers, the treatment of the cavitation in these bearings lags far behind that for the simpler journal bearings. To date cavitation in squeeze film dampers is treated by assuming a π-film model which neglects altogether the negative pressure region. This model is often referred to as "unpressurized," while the term "pressurized" refers to the 2π-film model or the uncavitated case. Furthermore, the pressure in the circumferential feed groove is often assumed constant and set equal to zero or equal to the supply pressure. The intent of this paper is to investigate these underlying assumptions and check their validity. It is also hoped that a better understanding will emerge from identifying the various forms of cavitation that can take place in a squeeze film damper bearing.

EXPERIMENTAL APPARATUS

Experimental test rigs utilized in the study of squeeze film dampers have for the most part been low speed and of large clearances mainly for the convenience of such designs in the laboratory and in order to reduce the dynamic effects inherent in high speed operation. San Andres and Vance [11] used a low speed test rig with a large clearance to investigate the inertial effects of the squeeze film. The new test rig utilized in the current investigation is an outgrowth of the

previous apparatus, and was designed to operate at higher speeds incorporating a clearance closer to industry practice in order to determine if there are variables pertinent to high speed operation that have not been adequately simulated by the lower speed test rig.

The test rig is shown in figure 1. It consists of a rigid shaft supported on three super precision angular contact ball bearings with the squeeze film journal mounted on an eccentric piece to provide a controlled orbit. The shaft is driven by a variable speed DC motor through a toothed belt at speeds up to 5000 rpm. Oil is introduced to the circumferential feed groove through four inlet holes 2.38 mm (3/32 in) in diameter and located 90 degrees apart. A solid piston ring prevents leakage out of the feed groove with two serrated piston rings located at the inlet and outlet of the squeeze film land and are shown in figure 2. The serrated piston rings allow adequate flow through the damper and prevent distortion of the pressure wave normally experienced with the presence of inlet and outlet holes. They also produce higher pressures in the film than an open end. The journal is 166 mm (6.539 in) in diameter and 25.4 mm (1 in) long with a radial clearance of 0.635 mm (0.025 in) and an operating eccentricity of 0.45.

IDENTIFICATION OF CAVITATION REGIMES

The dynamic oil pressure is measured using piezoelectric pressure transducers located axially and circumferentially around the housing or outer ring. In the early stages of this study it was desired to obtain an overall view of the characteristics exhibited by this test rig throughout its operating speed range. To accomplish this in a fast and efficient way, the peak to peak pressures were obtained from a digital vector filter (DVF-2) as a function of speed and are shown in figure 3. The oil flow for this measurement was kept around (0.4 gal/min), a value determined by the heat transfer requirements for a typical squeeze film damper configuration. This pressure measurement identified three distinct regions of operation. The lowest speed region has the damper operating uncavitated. The second regime shows a slight drop in the slope of the pressure curve which is attributed to the presence of cavitation in the damper. The last region shows a drastic drop in pressure and an erratic signal. Based on observations of the oil condition at the outlet of the damper, this behaviour is attributed to a bubbly mixture of air and oil.

The characteristic exhibited in this measurement prompted a flow visualization experiment in order to verify the hypothesis just presented and to further clarify the type and extent of cavitation that takes place in a squeeze film damper bearing. Details of the flow visualization experiment were reported in reference [12]. Once the different regimes were identified through the use of high speed photography, pressure measurements were obtained at conditions that corre-

sponded to these regimes in order to outline and characterize the qualitative visualization experiment by quantitative pressure measurements.

Regime I- uncavitated 2π-film: This region is characterized by a full film in the bearing with no apparent film rupture. Operation in this regime takes place when the test rig is operated in the low speed range, or at small orbit eccentricities. It is also possible to achieve an uncavitated operation provided the supply pressure is increased to at least the peak pressure in the oil film and arranged so as to prevent the entrainment of atmospheric air into the damper. A pressure wave characteristic of operation in this regime is shown in figure 4. The pressure signal shows no discontinuity and is characterized by a slightly larger negative pressure region. Integration of the pressure along and perpendicular to the line of centers verifies the presence of a radial force directed outwards, and this has been attributed to the effect of fluid inertia in the damper [11]. The possibility for an engine to operate in such a regime with contemporary bearing configurations and available supply pressures is considerably remote. In spite of the limited need for the analysis of a damper operating in this regime, the efforts have been numerous mainly due to the simplicity such a model provides, and in many cases to highlight special effects such as those of fluid inertia where uncavitated operation facilitates the separation of damping and inertial coefficients.

Regime II- cavitation bubble following the journal: In this regime a ventilated cavity bubble forms and follows the journal around without affecting the positive pressure region. Cole and Hughes [5] witnessed such a behaviour on a dynamically loaded journal bearing operating at a relatively low speed. This evidence has been relied upon to treat cavitation in dynamically loaded journal bearings in a similar manner to that in steadily loaded journal bearings. Figure 5 shows a photograph that identifies such a regime in a squeeze film damper bearing when operated at a low speed, and an inlet oil flow of 0.4 gal/min. This flow corresponded to an inlet supply pressure of 3 psig which allowed air to enter the damper when the negative pressure exceeded that value. A pressure measurement which corresponds to operation in this regime is shown in figure 6. The pressure in the positive region is not affected by the presence of the cavitation bubble. This was also confirmed by the flow visualization experiments which did not reveal the presence of any bubbles in the positive portion of the cycle. The operation in this regime can occur in low speed dynamically loaded bearings, but in the case of squeeze film damper bearings this would more appropriately represent a transition regime as the engine is accelerated to full speed. The persistence of this regime once steady state conditions have been reached are considerably remote.

Regime III- oil-air mixture: As speed is further increased transition from regime II to regime III takes place. The higher speed operation traps portions of

the air bubble, and in the presence of the higher pressure region the bubbles will breakup into smaller cavities or diffuse into the oil. The higher speed operation results in larger negative pressures which means the entrainment of greater amounts of air into the damper. The air bubbles do not collapse as vapor bubbles do, but compress and reduce in size as evident by the photograph shown in figure 7. This ultimately results in a reduction of the pressure amplitude. The size and amount of bubbles are found to be very much speed and pressure dependent. The higher the speeds and pressures, the finer and more numerous the bubbles are. The fluid content in the positive region of the cycle mainly consists of a cloudy oil mixture of finely dispersed air bubbles, and fewer large patches of air cavities. In the negative pressure region, the fine air bubbles and the larger air cavities coalesce and expand to form larger cavities. The presence of air bubbles in this region prevent the oil from achieving the high negative pressure values it would otherwise attain. A pure oil in the absence of air cavities would sustain a larger tensile force until vaporization can take place. Figure 8 shows a pressure measurement that is representative of operation in this regime. One of the distinguishing features is of course the relatively low positive pressure amplitude, but of more importance is the reduced circumferential extent of the positive pressure region. Another feature of importance is a phase shift of the positive pressure peak further downstream, and a delay in the buildup of the positive pressure which is attributed to the presence of the compressible air bubbles as evident in the flow visualization experiment. The negative pressure region occupies a much larger extent as compared to the uncavitated case. It is the authors' belief that the majority of current squeeze film dampers inevitably operate in such a regime considering the supply pressure and flows that are typical of existing squeeze film damper applications.

Parkins and May-Miller [13] utilizing two flat plates with the top plate oscillating normal to the oil film identified a regime which had some similarities to the one just described. They referred to this type of cavitation as a cavitation regime with bubbles fed from outside the film.

Regime IV- vapor cavitation: It is possible to operate in this regime if the end seals have a very tight configuration so as to prevent the ingress of air from the atmosphere, and provided the supply pressure is just below the peak pressure in the film. In order to simulate this condition, the supply pressure to the damper was increased from the 3 psig level utilized in generating the previous regime to 25 psig. This served to prevent air bubbles from entering the damper, and allowed the negative pressure to reach the vapor pressure level during a certain speed range. Figure 9 shows a of photograph obtained from the high speed visualization experiment which provided a good indication of the circumferential and axial extent of the vapor cavitation regime. The vapor cavities exist only during the negative portion of the cycle and are seen to immediately collapse as soon as the local pressure increases beyound the vapor pressure of the oil. Thus

their influence is limited to the negative pressure region and does not affect the positive pressure region, a fact that was confirmed by the pressure measurements which corresponded to operation in this regime as shown in figure 10. The pressure signal shows a flat horizontal response once the vapor cavitation has been reached. As the vapor bubble collapses, the pressure immediately resumes the value it is predicted to attain. To further highlight the distinctive features of this regime and that of regime III, additional measurements were carried out as shown in figure 11. In this set-up the test rig was run at 4000 rpm in both cases but with a supply pressure of 40 and 25 psig respectively. The case with the 40 psig simulated the vapor cavitation case, and clearly showed the effect the vapor collapse has on the pressure measurement which was evident by the overshoot in the pressure as a result of the implosion that takes place. It is this phenomenon which is associated with vapor cavitation that causes damage to bearing surfaces resulting in pitting marks. The positive and negative regions in this case occupy equal circumferential extents, unlike the gaseous cavitated case where the negative pressure occupies almost three quarters of the cycle. The gaseous cavitation case shows a lower positive amplitude, and a delay in the buildup of the pressure region, in addition to a shift in phase of the peak pressure as compared to that of the vapor cavitation case. The presence of bubbles in the gaseous cavitation case prevented the negative pressure from achieving the value of the vapor pressure. Walton et al.[14] were able to produce vapor cavitation in a damper bearing through the use of Teflon backup rings to provide tight sealing.

Regime V– vapor and gaseous cavitation: This regime follows directly from the previous regime as the speed is further increased until the peak pressure in the film exceeds the oil supply pressure thus drawing in air bubbles from the atmosphere due to the pressure drop across the seals. In this regime vapor cavitation takes place first, followed by the ingress of air into the bearing. The photograph shown in figure 12 illustrates the conditions in the negative portion of the cycle where the trailing edge of the vapor cavity is seen to collapse at the same time air bubbles are being drawn into the damper. This also demonstrates the ability of the air bubbles to withstand the high pressure region where they are seen to shrink in size but continue to exist throughout the high pressure region of the cycle. As the speed is further increased more air bubbles enter the damper and interfere with the vapor bubble collapse reducing the effect of the implosions as shown in the pressure wave of figure 13. In this figure vapor cavitation is noted first as indicated by the flat portion of the negative pressure followed by a slight reduction in the negative pressure caused by the ingress of air into the damper. The ingress of air bubbles delays the increase of positive pressure, and eliminates the overshoot that was associated with the implosion. This last effect seems favorable however, and has been used to advantage in certain applications [15] to reduce the severity of vapor cavitation which normally results in rapid pitting and errosion of adjacent surfaces. Further increase in speed increased

the amount of air bubbles in the fluid untill there was enough air to completely prevent the formation of vapor cavitation, thus in effect transforming this regime to that of regime III which was dominated by gaseous cavitation effects.

EFFECTS OF SUPPLY PRESSURE

The conditions which determine the type of cavitation regime a squeeze film damper operates in depends on many design parameters which include the type of seals and their effectiveness, the speed and operating eccentricity, and most importantly the supply pressure. A squeeze film damper bearing features a non-rotating journal, and so differs considerably from journal bearings and dynamically loaded bearings. The pressure normally generated in all types of bearings causes oil to be expelled from the bearing. In the case of journal bearings, the oil is drawn into the high pressure region of the film by viscous shear at the surface of the spinning journal. In dynamically loaded journal bearings which normally operate in a flooded reservoir, oil is introduced by the spinning journal as was described for journal bearings. In addition, the dynamic motion results in separation of the bearing surfaces during a part of the cycle, and as they do so they draw oil into the bearing lands from the sides since no end seals are utilized with this type of bearings. This mechanism with the exception of rotation is similar to that in squeeze film damper bearings, but these do not normally operate in a flooded reservoir and are usually equipped with end seals. This leaves the oil supply pressure as the only means of introducing oil into such a bearing. Thus it is not surprising to learn how critical the supply pressure is on the performance of squeeze film dampers. Despite the importance of the supply pressure, some investigators including the authors have treated it superficially, and addressed the effects of pressurization by considering its two extremes. The term "pressurized" is often used to indicate an uncavitated bearing, while the term "unpressurized" is used to imply a π-film model, a condition that is similar to that described in regime IV with the additional simplification of neglecting all the negative pressure region. The justification given for neglecting this region which extends from zero pressure to about -35 psig, relies on the assumption that the positive pressure region in actual engine applications which operate at higher speeds and lower clearances extrapolates to positive peak pressure values in the range of 500 to 1000 psig. This would render the negative pressure region negligible in comparison. Simandiri and Hahn [16] have recognized the effect of pressurization on the squeeze film damper, notably the elimination of the jump phenomenon once the pressure was increased to prevent the bearing from operating in a cavitated condition. They cite an equation from which one can determine the required supply pressure to achieve the uncavitated operation. However, these pressures in the case of a typical engine configuration translate to a supply pressure in excess of 500 to 1000 psig, while most existing installations

are only capable of providing pressures in the range of a few psig to about 60 or 80 psig. The required high pressures will also result in excessive flows which the present scavenge pump installation would have difficulty in handling. Operation in the uncavitated region is particularly unattractive for squeeze film dampers that are not equipped with a centering spring, since the damper in this case would have to be relied upon to provide or generate the stiffness required for the load carrying capability as demonstrated by Holmes and Humes [17].

Based on these current limitations, a cavitated damper is the most probable model to consider for existing squeeze film damper installations. The question however, is to determine the type of cavitation and the effect different supply pressures have on the dynamic pressure and the resulting radial and tangential forces. A plot of the dynamic peak to peak pressure for three different inlet pressures is shown in figure 14. Unlike the plot in figure 3 this figure was obtained by taking measurements at discrete speeds, however the general trend and characteristics remained the same. The transition to the bubbly region is still evident by the characteristic knee shape of the pressure curve, which occurs at a speed of approximately 1500 rpm for the case of 3 psig supply pressure. The upper two curves are for the supply pressures of 8 and 25 psig respectively. The net effect of increasing the pressure is to cause a shift in the characteristic knee shape of the pressure curves up in speed. Increasing the supply pressure delays the onset of gaseous cavitation regime or "bubbly region", but it is always reached as speed is increased or when the test rig is operated at higher eccentricities. The supply pressure should theoretically have no effect on the dynamic pressure, and this is actually reflected in the plots at the low speed range where all three cases of supply pressures result in uncavitated regimes. The influence of the supply pressure becomes more apparent as speed is increased and the cavitation extent is expanded. The dynamic pressure in the feed groove was also measured and is shown in the lower three curves of figure 14. The groove pressure reflects the variations of pressure in the squeeze film land indicating that the commonly utilized assumption of constant pressure in the feed groove is not appropriate. The pressures in the feed groove seem to follow the pressures in the squeeze film land, despite the fact that in this damper configuration a serrated piston ring is placed between the feed groove and the squeeze film land. The flow visualization experiments provide a clue to explain the mechanism by which the pressure in the feed groove can reach these unpredicted values. The high speed motion pictures reveal that axial flow from the squeeze film land into the groove is the major contributing factor. The oil exits the squeeze film land at a relatively high axial velocity and is decelerated as it enters the larger clearance in the feed groove. The velocity head transforms into a pressure head at the interface and causes the pressure increase in the feed groove.

CAVITATION EFFECTS ON THE SQUEEZE FILM FORCES

The radial and tangential forces are obtained by integration of the measured pressures along and across the line of centers. The radial and tangential damping coefficients can then be derived from these forces as shown in the Appendix. For the case of an uncavitated damper executing a circular centered orbit, the cross coupled damping and inertia terms are zero. This allows straight forward evaluation of the direct inertia and direct damping coefficients from the radial and tangential forces respectively. For the case of a cavitated damper it is not possible to separate the inertia and damping coefficients. Instead, equivalent radial and tangential damping coefficients are defined, noting that the radial coefficient represents the effect of the direct inertia plus the cross coupled damping term, while the tangential coefficient represents the direct damping plus the cross coupled inertia term. Figure 15 shows a plot of the radial and tangential dimensionless coefficients for the three different cases of supply pressure. While in the uncavitated regimes the tangential coefficient is more or less constant, the effect of gaseous cavitation is to reduce it drastically. The traditional π-film model predicts damping coefficients of half the value obtained from the 2π-film model. This does not seem to be reflected by these measurements as operation progresses from uncavitated to cavitated conditions . The inertial coefficient which is the only term contributing to the radial force in the uncavitated region is soon negated by the cross coupled damping term which dominates as the cavitation extent in the damper increases. This fact is further verified by calculating the phase angle from the measured radial and tangential force components. The phase angle, which represents the angle between the total damper force and the line of centers measured from location of maximum film thickness, was obtained using equation (A10) for the three supply presure cases as shown in figure 16. In all three cases, a phase angle larger than 90 degrees is obtained when operating in the uncavitated region indicating that the radial force is directed outwards. As air enters the bearing, the gaseous cavitation effects increase. This tends to shift the phase angle from above 90 degrees to around 50 to 60 degrees depending on the extent and amount of gaseous cavities present. The radial force at this instant has reversed directions and is oriented inwards. It is interesting to note that the curve for the supply pressure of 25 psig showed a region of vapor cavitation in which the phase angle was actually above 90 degrees and increasing just as was the case for the uncavitated regime. This is one more feature that distinguishes the two types of cavitation and is shown schematically in figure 17. It is of interest to further check the phase angle for the forces in the feed groove and see whether they are in phase with the forces in the squeeze film land. The phase in the squeeze film land and feed groove for the case of 8 psig supply pressure is shown in figure 18. We note that the difference is minimal in the uncavitated region, but as gaseous cavitation increases the phase shift in the squeeze film land deviates further because the

gaseous cavities occupy a larger portion of the total fluid in this region than those in the feed groove.

CONCLUSION

The cavitation regimes in a squeeze film damper bearing are much more complex and varied in nature than those for journal and dynamically loaded bearings. Five distinct operating regimes were identified through the use of high-speed motion pictures, and were subsequently characterized through pressure measurements. A proper transient analysis requires adequate modeling of the fluid film forces corresponding to each regime. This requirement further highlights the inadequacy of the π-film model for transient analysis.

Air entrainment was shown to drastically modify the pressure wave. Its effect is to reduce the negative pressure amplitude and prevent vapor cavitation from taking place. The circumferential extent of the negative pressure is enlarged, and subsequently the positive pressure region is reduced. The delay of the positive pressure buildup is attributed to the presence of bubbles. The bubbles are also responsible for the reduction of the positive pressure amplitude. While in the uncavitated and vapor cavitation regimes, the measured force has a phase angle of larger than 90 degrees. The effect of gaseous cavitation is to shift the peak pressure further downstream and results in phase angles smaller than 90 degrees. This effect is opposite to that of fluid inertia.

The pressure in the groove was verified to be a direct consequence of the axial flow from the squeeze film land into the groove.

This investigation highlights ways that existing squeeze film dampers could be improved. The oil feed mechanism, seals, and outlet holes, in addition to the supply pressure could be modified to reduce the entrainment of air into the bearing and to enhance damper performance.

APPENDIX

For a squeeze film journal executing a circular centered orbit, the radial and tangential forces can be obtained by integration of the pressure wave,

$$fr = \int_0^1 \oint P cos\theta \, d\theta \, d\beta \tag{A1}$$

$$ft = \int_0^1 \oint P sin\theta \, d\theta \, d\beta \tag{A2}$$

where P=$\mu \omega R^2/c^2$ Dimensionless pressure

$$fr = -Cr.\omega \tag{A3}$$

$$ft = -Ct.\omega \tag{A4}$$

where

$$Cr = Crt - Drr\omega \tag{A5}$$

$$Ct = Ctt + Dtr\omega \tag{A6}$$

for the case of an uncavitated damper Crt=Dtr=0
and

$$Cr = -Drr\omega \tag{A7}$$

$$Ct = Ctt \tag{A8}$$

The total film force:

$$F_i = [(fr_i)^2 + (ft_i)^2]^{1/2} \tag{A9}$$

and the force phase angle:

$$\phi_i = 90 + \tan^{-1}(fr_i/ft_i) \tag{A10}$$

measured from maximum gap location.

REFERENCES

[1] Mohan, S., and Hahn, E. J., "Design of Squeeze Film Damper Supports for Rigid Rotors," *Journal of Engineering for Industry, Trans.* **ASME**, Vol. 96, No.3, 1974, pp. 976–982.

[2] Rabinowitz, M. D., and Hahn, E. J., "Steady State Performance of Squeeze Film Damper Supported Flexible Rotors," *Journal of Engineering for Power, Trans.* **ASME**, 99, 4, pp. 552–558 (1977).

[3] Hahn, E. J.,"Stability and Unbalance Response of Centrally Preloaded Rotors Mounted in Journal and Squeeze Film Bearings," *Journal of Lubrication Tech., Trans.* **ASME**, 101, 2, pp. 976–982 (1979).

[4] Nikolajsen, J. L. and Holmes, R., "Investigations of Squeeze-film Isolators for the Vibration, Control of a Flexible Rotor," *J. Mech. Eng. Sci.* (1979).

[5] Cole, J. A. and Hughes, C. J., "Visual Study of Film Extent in Dynamically Loaded Complete Journal Bearings," *Proc. Lub. Wear Conf.* 1957 , (I. Mech. E.) 147–149.

[6] White, D. C., "Squeeze Film Journal Bearings," Ph.D. dissertation. Cambridge University, December 1970.

[7] Hibner, D. H., and Bansal, P. N., "Effects of Fluid Compressibility on Viscous Damper Characteristics", Proceedings of the Conference on The Stability and Dynamic Response of Rotors with Squeeze Film Bearings, University of Virginia, 1979.

[8] Thomsen, K. K., and Andersen, H., "Experimental Investigation of a Simple Squeeze Film Damper," **ASME** Paper No. 73-DET-101.

[9] Botman, M., "Experiments on Oil-Film Dampers for Turbomachinery," *Journal of Engineering for Power, Trans.* **ASME**, Series A, Vol. 98, No. 3 July 1976, pp. 393–400.

[10] Sharma, R. K., "An Experimental Study of the Steady- State Response of Oil-Film Dampers," *Journal of Mechanical Design, Trans.* **ASME** Vol. 100, April 1978, pp. 216–221.

[11] San Andres, L. A., and Vance, J. M., "Experimental Measurement of The Dynamic Pressure Distribution in a Squeeze Film Damper Executing Circular- Centered Orbits," **ASLE** Trans. Vol. 30, No. 3, July 1987.

[12] Zeidan, F. Y., and Vance, J. M., "Cavitation Leading to a Two Phase Fluid in a Squeeze Film Damper," Accepted for presentation at the STLE Annual meeting , Cleveland, Ohio, May 1988.

[13] Parkins, D. W., and May-Miller, R., "Cavitation in an Oscillatory Oil Squeeze Film," *Journal of Tribology, Trans.* **ASME**, Vol. 106, July 1984, pp. 360–367.

[14] Walton, J., Walowit, E., Zorzi, E. and Schrand, J., "Experimental Observation of Cavitating Squeeze Film Dampers," **ASME** Trans., Vol. 109, April 1987, pp. 290–295.

[15] Ramussen, R. E. H., "Some Experiments on Cavitation Erosion in Water Mixed with Air," **NPL** Symp. Cavitation in Hydrodynamics, 20 HMSO 1956.

[16] Simandiri, S., and Hahn, E. J., "Effect of Pressurization on the Vibration Isolation Capability of Squeeze Film Bearings," *Journal of Engineering for Industry, Trans.* **ASME**, Feb. 1976, pp. 109–117.

[17] Holmes, R., and Humes, B., "An Investigation of Vibration Dampers in Gas- turbine Engines," Proc. 52nd AGARD Symp., Cleveland, U.S.A. (Oct. 1978).

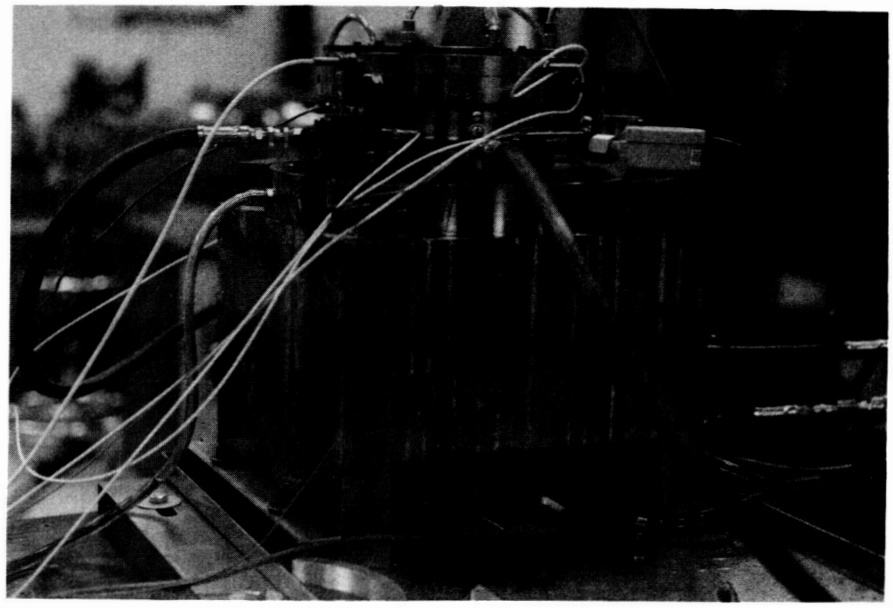

Figure 1: Controlled Orbit Squeeze Film Damper Test Rig.

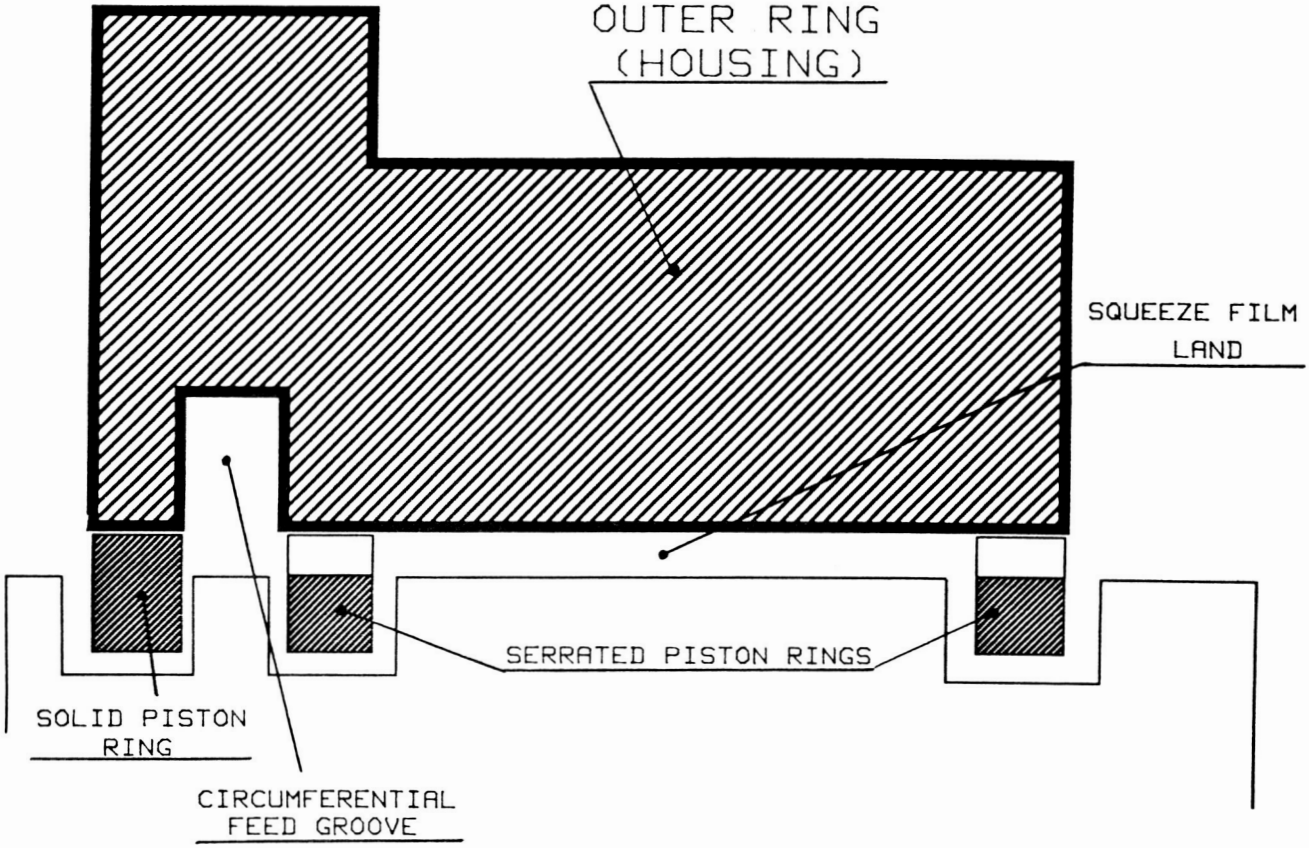

Figure 2: Schematic of Damper Configuration.

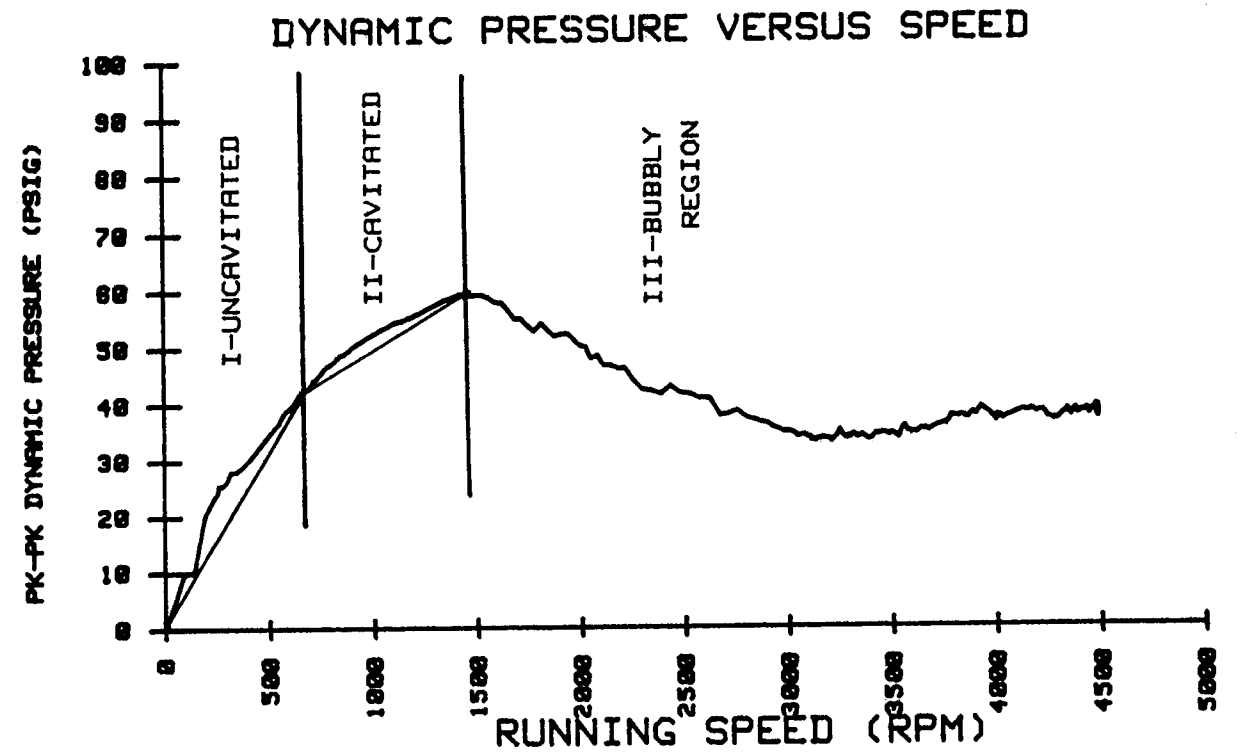

Figure 3: Peak to Peak Pressures vs Speed Identifying Three Distinct Regions of Operation at a Flow of 1.5 L/min (0.4 gal/min).

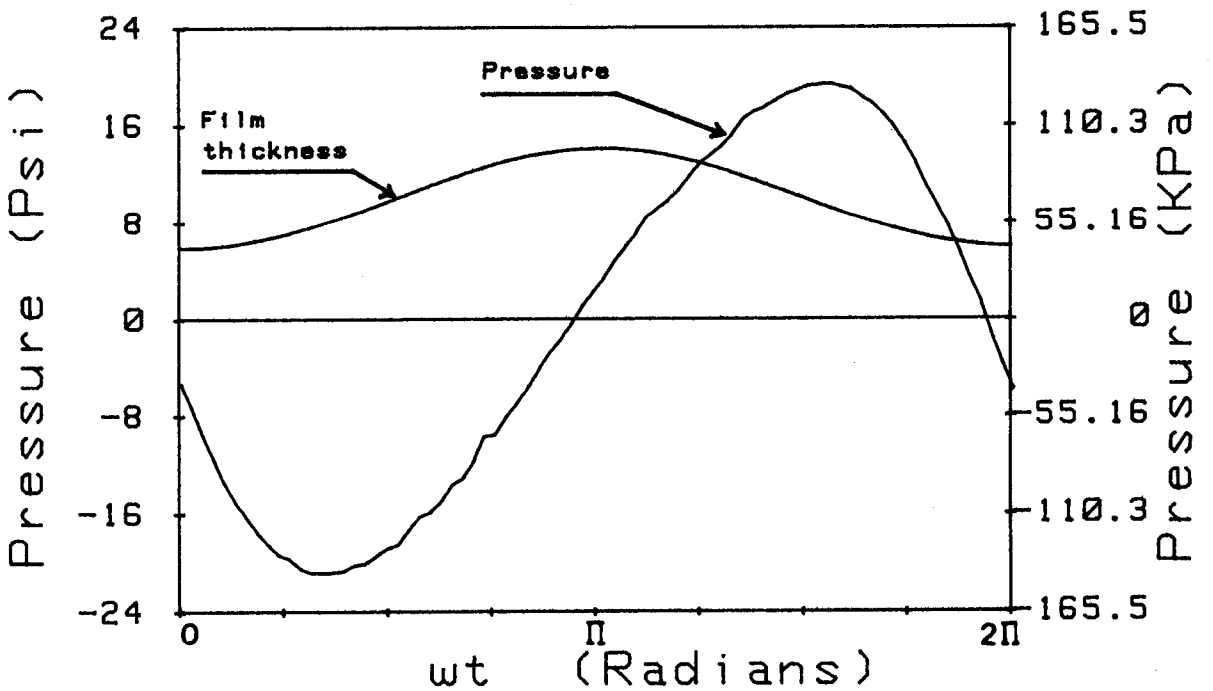

Figure 4: A Typical Uncavitated Pressure Wave.

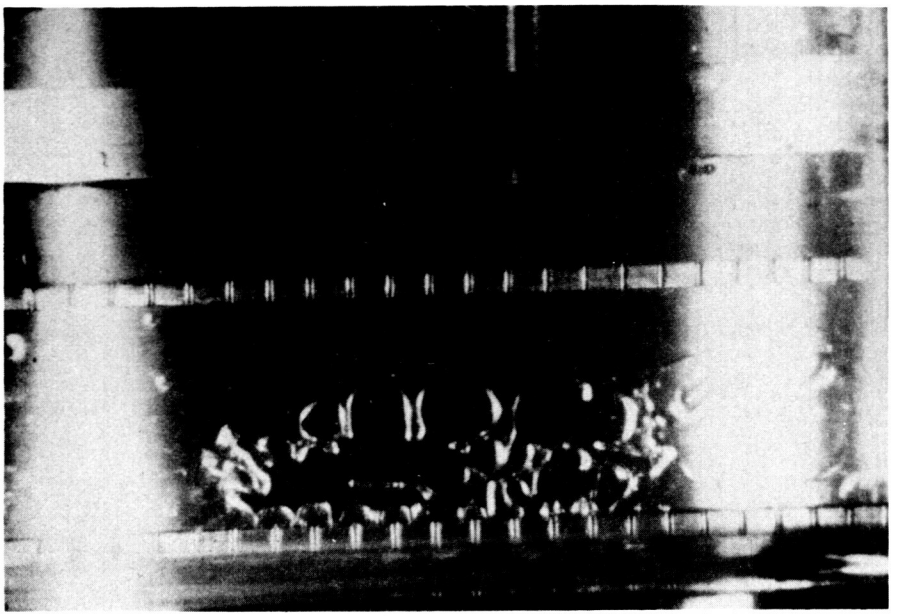

Figure 5: Gaseous Cavitation Bubble (A-A).

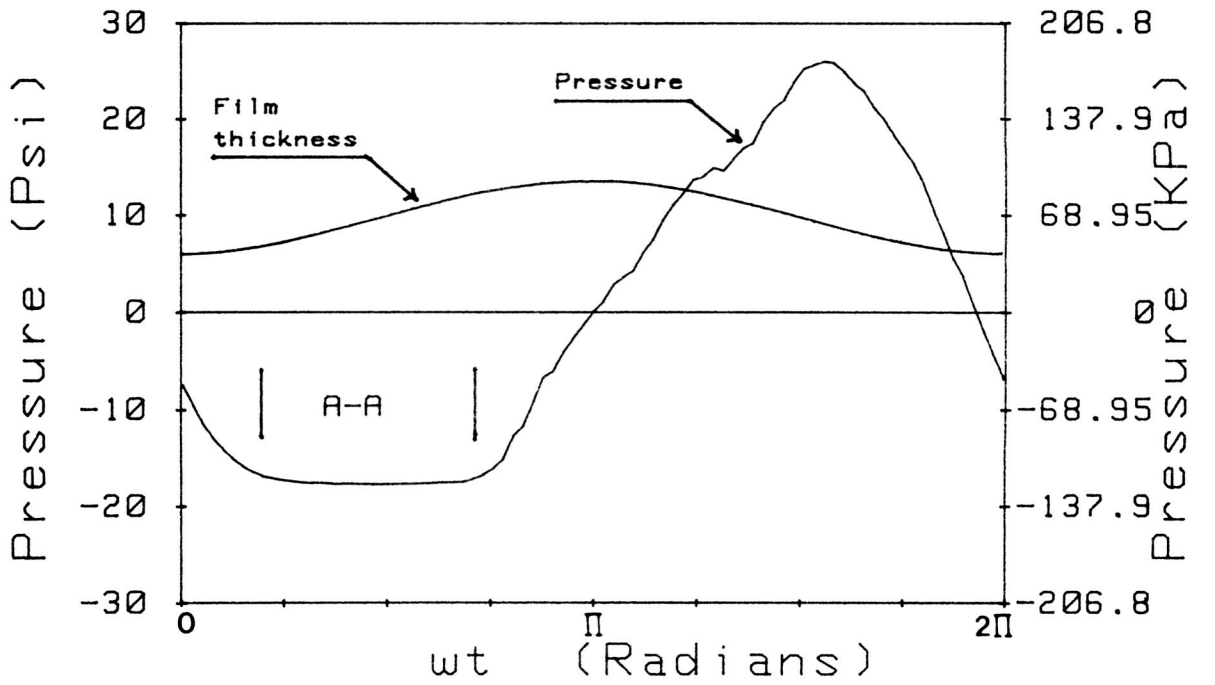

Figure 6: A Pressure Wave which Corresponds to The Cavitation Regime (II) shown in Fig. 5

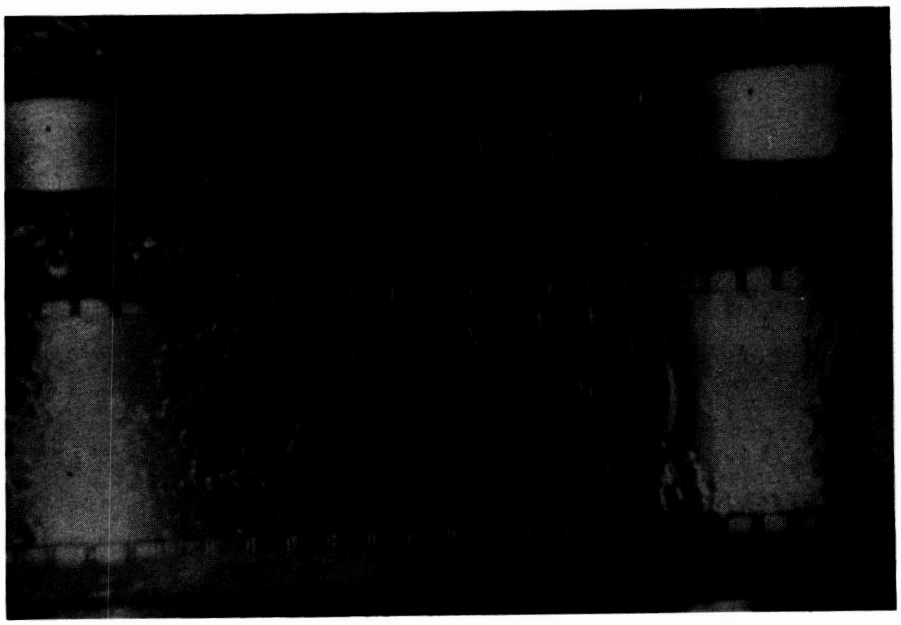

Figure 7: Air Bubbles in the High Pressure Region of Regime III.

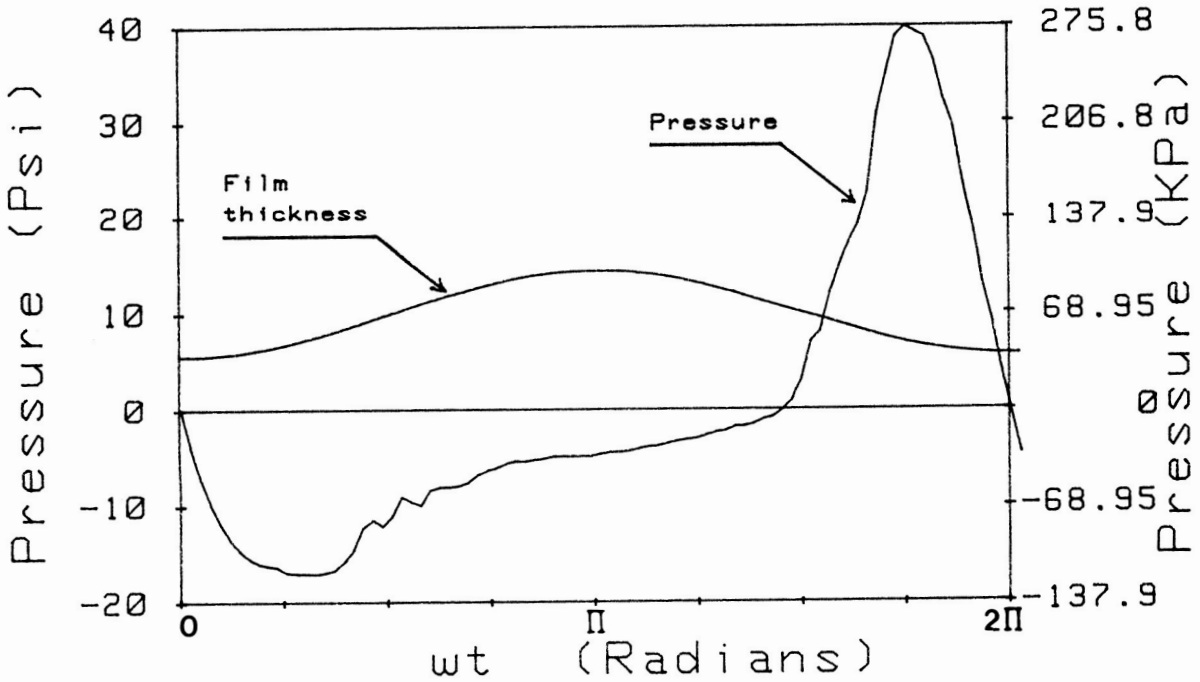

Figure 8: A Pressure Wave which Corresponds to The Gaseous Cavitation in Regime (III).

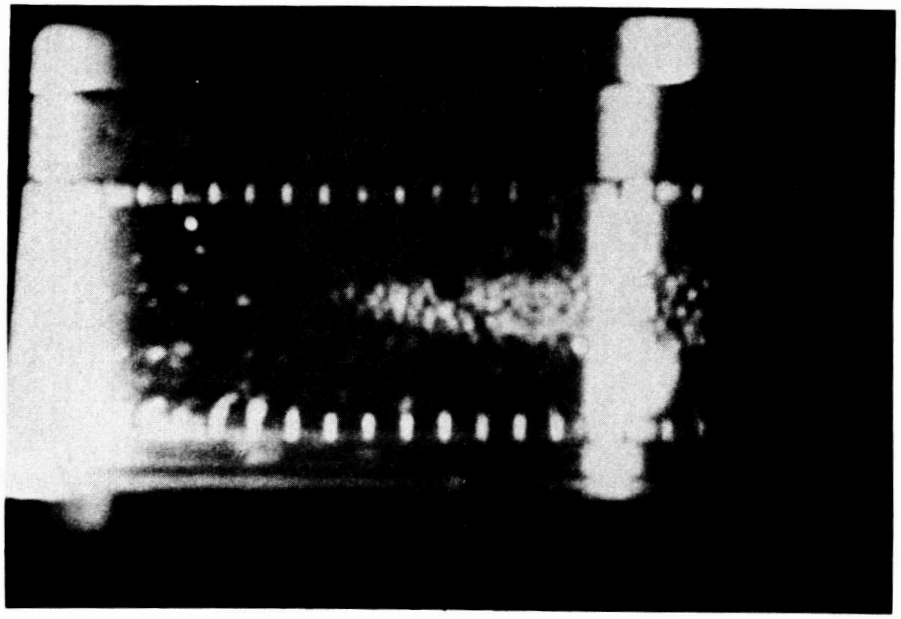

Figure 9: Vapor Cavitation in Regime (IV).

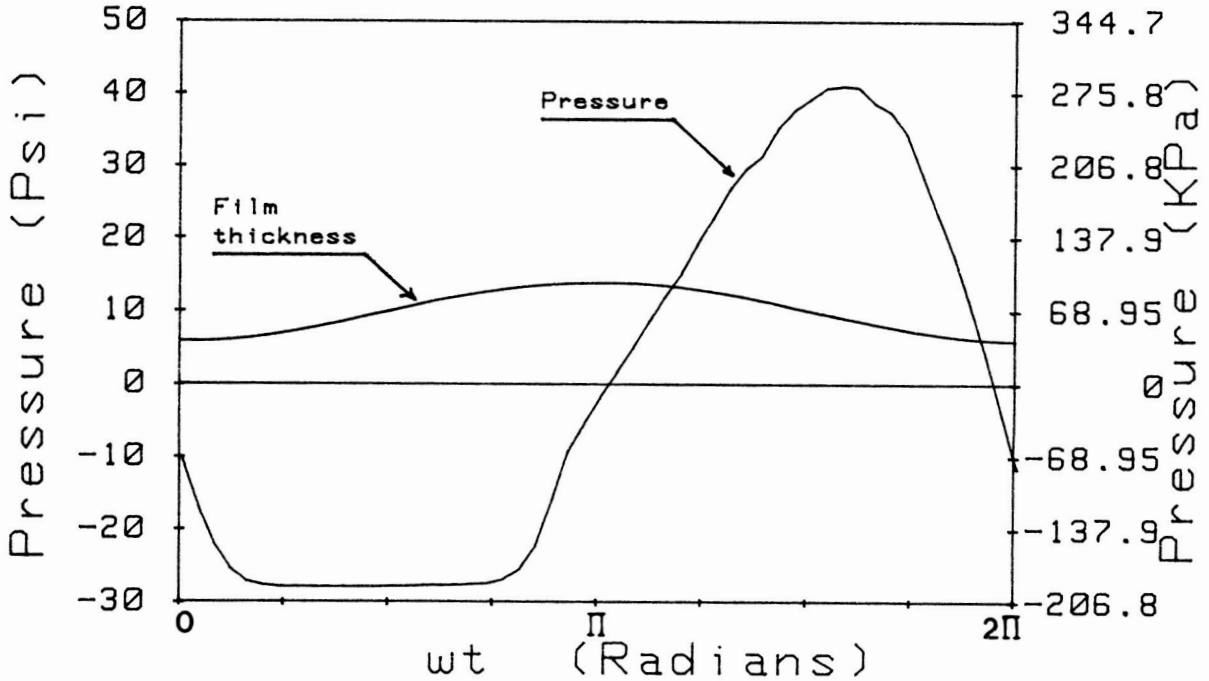

Figure 10: A Pressure Wave which Corresponds to The Vapor Cavitation in Regime (IV).

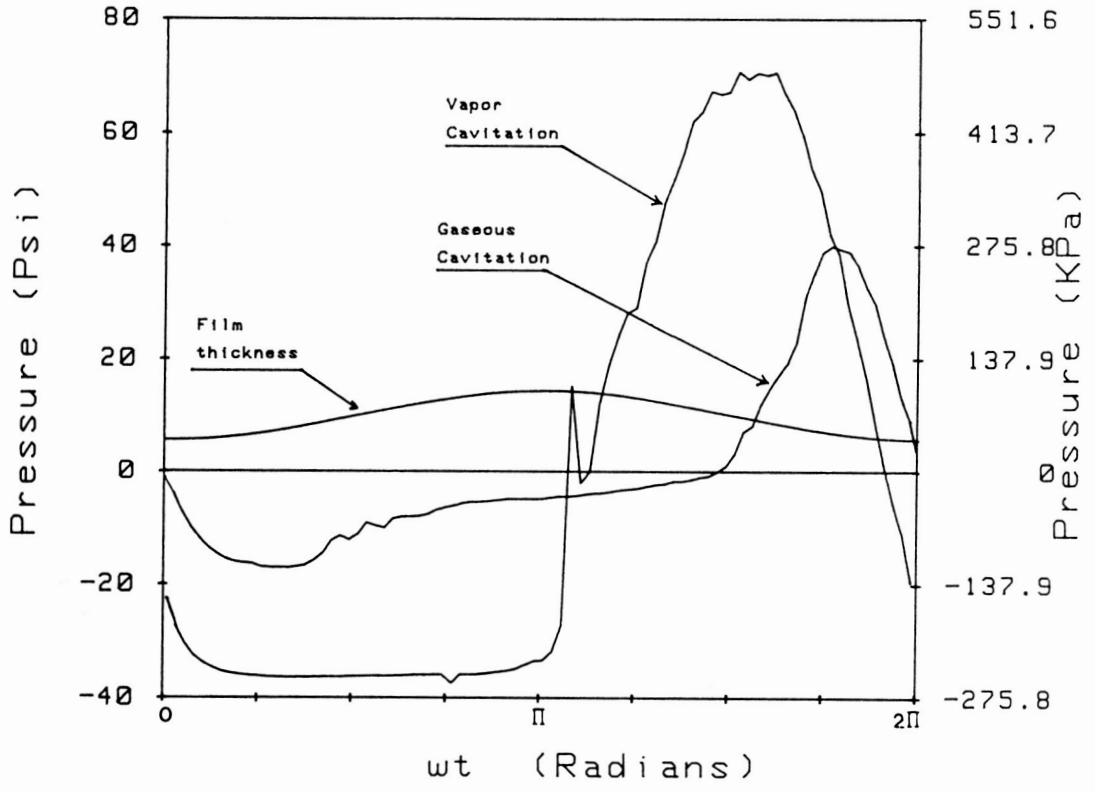

Figure 11: Comparison of Pressure Waves Corresponding to The Gaseous and Vapor Cavitation Regimes

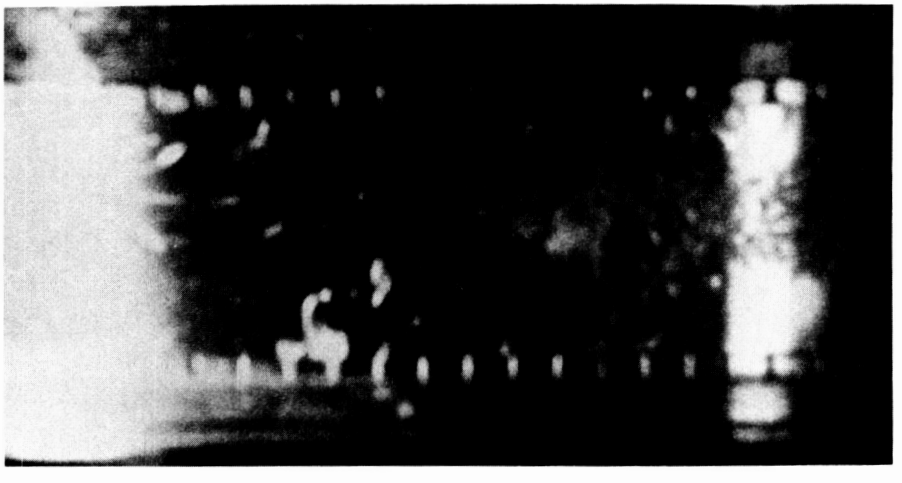

Figure 12: The Trailing End of the Vapor Cavitation Cloud is Shown as Air Bubbles just to the Left Enter Through the Piston Ring Seals.

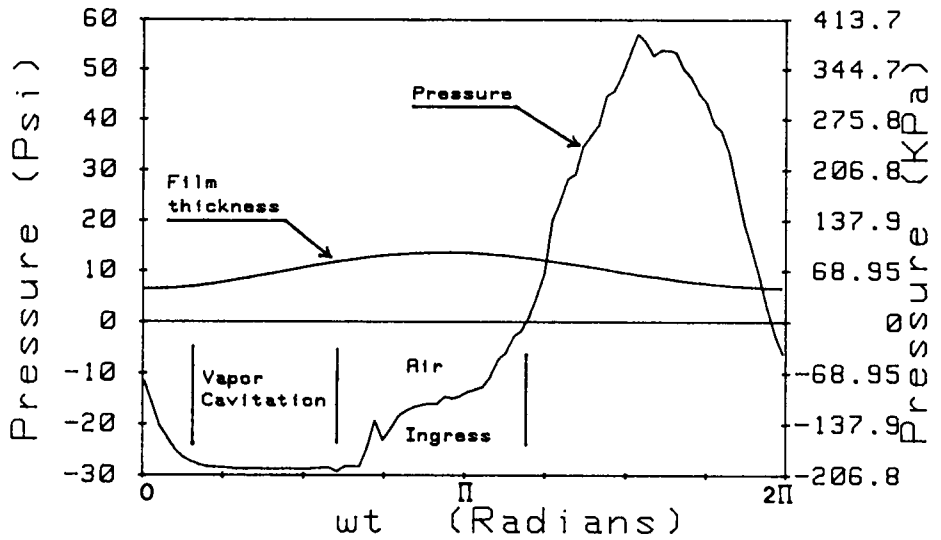

Figure 13: A Pressure Wave which Corresponds to The Vapor Plus Gaseous Cavitation in Regime (V).

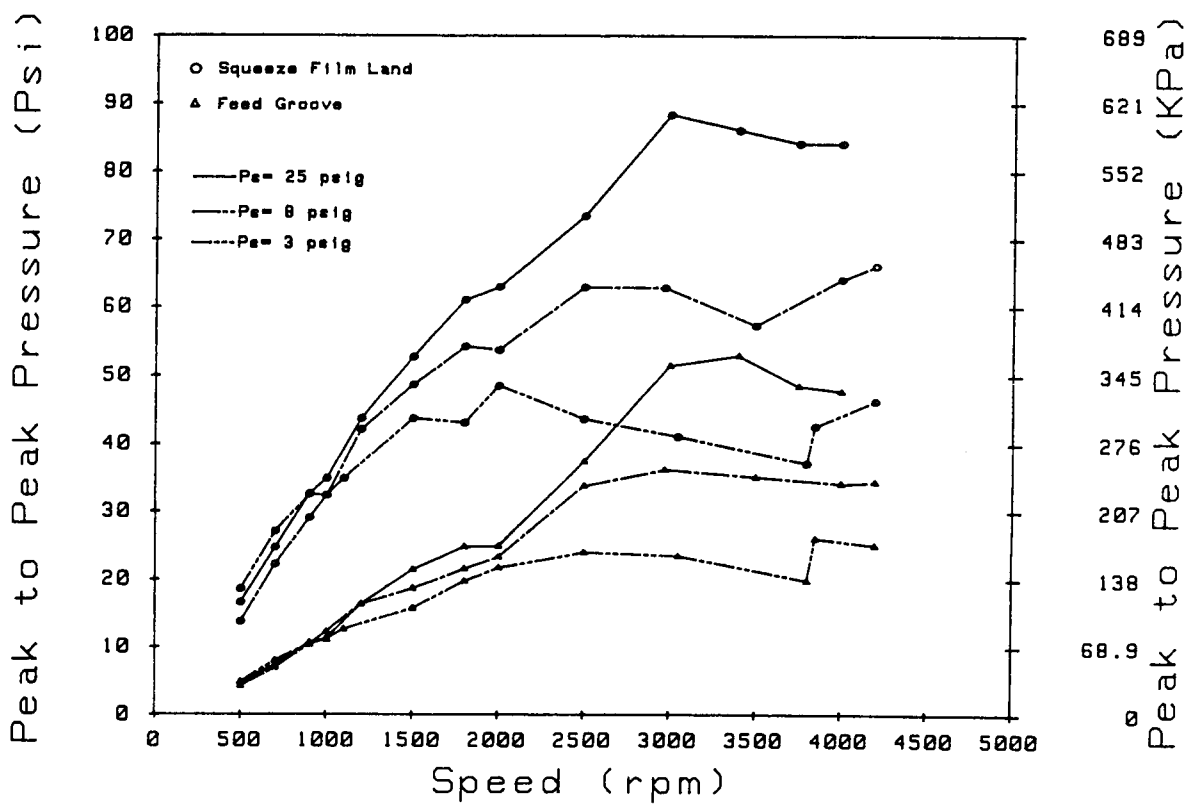

Figure 14: Measured pressures in the squeeze film land and Feed Groove at The Three Different Supply Pressures

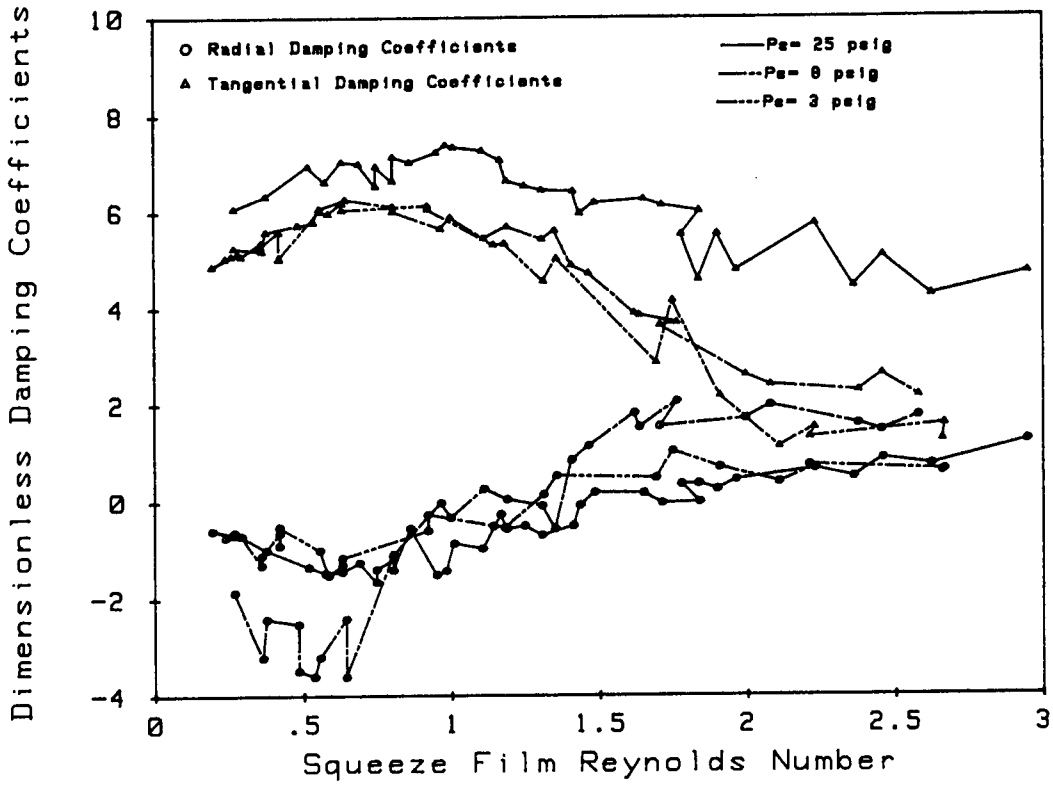

Figure 15: Dimensionless Damping Coefficients at The Three Different Supply Pressures

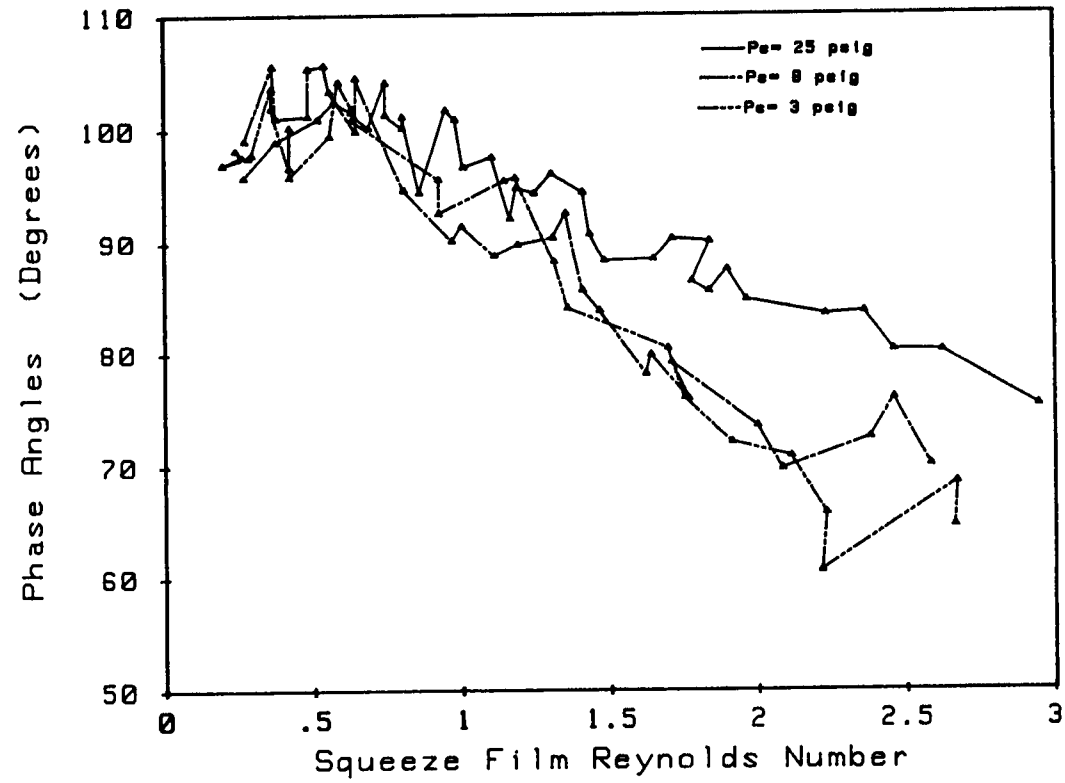

Figure 16: Phase Angles at The Three Different Supply Pressures

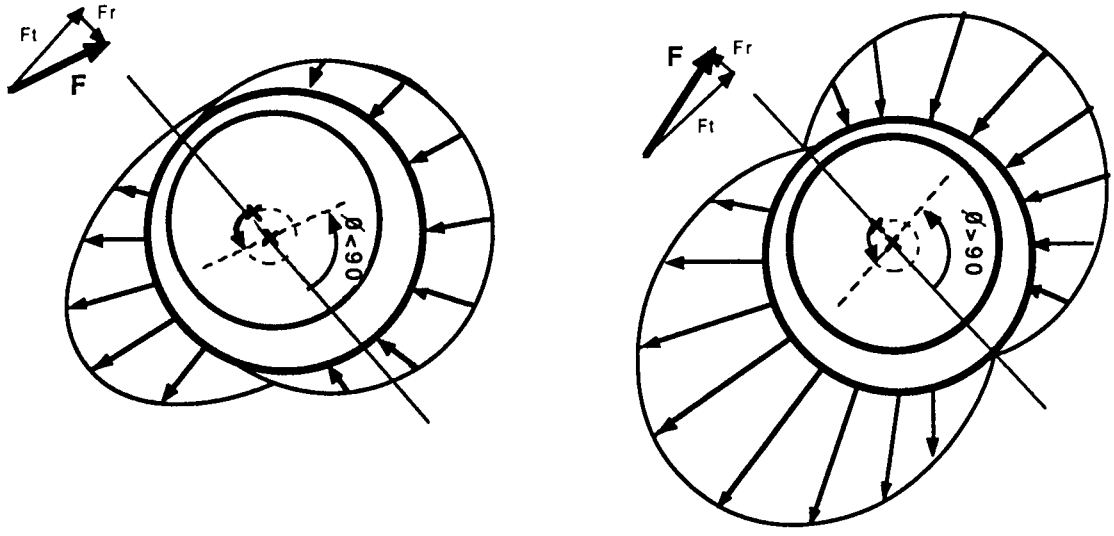

Gaseous Cavitation Case

Vapor Cavitation Case

Figure 17: A Comparison Between Gaseous and Vapor Cavitation Highlighting their Effect on the Pressure Distribution and Squeeze Film Forces.

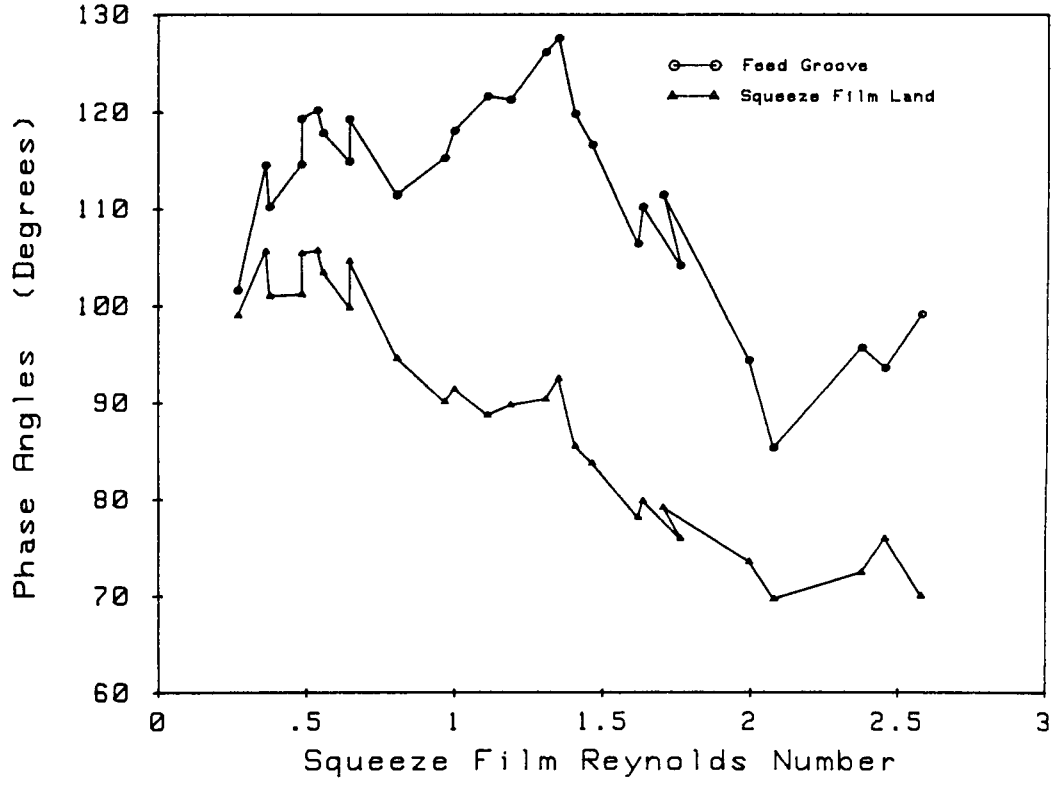

Figure 18: Phase Angles in the Squeeze Film Land and Feed Groove